International Journal of Nanomedicine

Dovepress
open access to scientific and medical research

Open Access Full Text Article

ORIGINAL RESEARCH

Enhancing Ezetimibe Anticancer Activity Through Development of Drug Nano-Micelles Formulations: A Promising Strategy Supported by Molecular Docking

Tarek A Ahmed[1], Ehab MM Ali[2], Abdelsattar M Omar[3], Alshaimaa M Almehmady[1], Khalid M El-Say[1]

[1]Department of Pharmaceutics, Faculty of Pharmacy, King Abdulaziz University, Jeddah, 21589, Kingdom of Saudi Arabia; [2]Department of Biochemistry, Faculty of Science, King Abdulaziz University, Jeddah, 21589, Kingdom of Saudi Arabia; [3]Department of Pharmaceutical Chemistry, Faculty of Pharmacy, King Abdulaziz University, Jeddah, 21589, Kingdom of Saudi Arabia

Correspondence: Tarek A Ahmed, Department of Pharmaceutics, Faculty of Pharmacy, King Abdulaziz University, Jeddah, 21589, Kingdom of Saudi Arabia, Tel +966 2 640 0000 Ext 22250, Email tabdelnapy@kau.edu.sa

Background: Ezetimibe, initially recognized as a cholesterol-lowering agent, has recently attracted attention due to its potential anticancer properties. We aimed to explore an innovative approach of enhancing the drug anticancer activity through the development of drug nano-formulations.

Materials and Methods: Fifteen different nano-micelles formulations were prepared utilizing D-α-tocopherol polyethylene glycol 1000 succinate (TPGS) and pluronic F127. The prepared formulations were characterized for size, polydispersity index (PDI), zeta potential, and entrapment efficiency (EE). The formulations were morphologically characterized using light and transmission electron microscopies and the drug-binding mode with the active site was investigated using the molecular docking. Cell viability against MCF-7 and T47D was studied. Apoptosis and cell cycle were assessed.

Results: The prepared formulations were in the nano-size range (34.01 ± 2.00–278.34 ± 9.11 nm), zeta potential values were very close to zero, and the TPGS-based micelles formulations showed the highest ezetimibe EE (94.03 ± 1.71%). Morphological study illustrated a well-defined, spherical nanoparticles with a uniform size distribution. Molecular docking demonstrated good interaction of ezetimibe with Interleukin-1 Beta Convertase through multiple hydrogen bonding, covalent bond, and hydrophobic interaction. TPGS-based nano-micelle formulation (F5) demonstrated the lowest IC_{50} against MCF-7 (4.51 µg/mL) and T47D (8.22 µg/mL) cancer cells. When T47D cells were treated with IC_{50} concentrations of F5, it exhibited significant inhibition with late apoptosis (43.9%), a response comparable to T47D cells treated with an IC_{50} dose of ezetimibe. Cell cycle analysis revealed that both ezetimibe and F5-treated T47D cells exhibited an increase in the subG1 phase, indicating reduced DNA content and cell death.

Conclusion: These findings suggest that F5 could serve as a proficient drug delivery system in augmenting the cytotoxic activity of ezetimibe against breast cancer.

Keywords: ezetimibe, TPGS, pluronic, micelles, anticancer activity, MCF7, T47D

Introduction

Cancer remains a global health concern and a leading cause of mortality worldwide. The development of effective therapies for combating cancer is a critical area of research, necessitating the exploration of novel drug candidates and repurposing existing medications. Ezetimibe is primarily known for its role as an inhibitor of intestinal cholesterol absorption through its interaction with the Niemann-Pick C1-like 1 (NPC1L1) transporter.[1,2] However, emerging preclinical and clinical data have suggested that ezetimibe may exhibit pleiotropic effects beyond its cholesterol-lowering activity, including potential anticancer properties. Recent in vitro and in vivo studies have demonstrated that ezetimibe exerts inhibitory effects on cancer cell proliferation, migration, and invasion. Moreover, it has been observed

Received: 12 September 2023
Accepted: 10 November 2023
Published: 15 November 2023

that ezetimibe can induce apoptosis, arrest the cell cycle, and inhibit angiogenesis in various cancer models.[3,4] These findings indicate a potential role for ezetimibe as an adjuvant therapy or a standalone treatment option in cancer management.[3] On the other hand, ezetimibe is characterized by its poor aqueous solubility (0.008 mg/mL) and low bioavailability. The drug undergoes significant metabolism in the intestine and liver before entering systemic circulation. Its bioavailability was reported to be around 35–65% due to extensive first-pass metabolism.[5] To enhance its solubility and bioavailability, various nanoformulations of ezetimibe have been investigated. Nanoformulations aim to improve drug delivery, absorption, and efficacy. Nanosuspensions,[6] nanoemulsions,[7] lipid-based nanoparticles,[8] and polymeric nanoparticles,[9] made from biodegradable polymers, such as poly(lactic-co-glycolic acid) or chitosan, have been utilized to overcome ezetimibe limitations or drawbacks associated with the drug. Although these nanoformulations of ezetimibe may have addressed certain limitations, there may still be a demand to enhance the overall efficacy of ezetimibe.

The mechanism underlying the anticancer activity of ezetimibe is not yet fully understood. It has been proposed that ezetimibe may affect cancer cell growth by modulating signaling pathways, including the Wnt/β-catenin pathway, which is crucial for cellular proliferation and survival. Additionally, ezetimibe's ability to inhibit the mevalonate pathway, involved in cholesterol biosynthesis and protein prenylation, may contribute to its anticancer effects.[4] Furthermore, the potential immunomodulatory properties of ezetimibe have been investigated,[10] suggesting a role in enhancing antitumor immune responses. In recent years, several studies have explored the therapeutic potential of ezetimibe in various cancer types, including breast, colorectal, lung, and pancreatic cancer.[3,11–14] These investigations have demonstrated promising results, suggesting that ezetimibe could be an effective therapeutic strategy for a broad range of malignancies. However, further research is necessary to elucidate the specific mechanisms and optimize treatment regimens to maximize its anticancer efficacy.

Effective drug delivery is crucial for optimizing therapeutic outcomes in various disease conditions. Over the years, considerable efforts have been made to develop novel drug delivery systems that can enhance drug solubility, stability, bioavailability, and therapeutic activity. Among these systems, micelles have emerged as versatile carriers with the potential to overcome numerous challenges associated with conventional drug formulations. D-α-tocopheryl polyethylene glycol succinate (TPGS), a water-soluble derivative of vitamin E, has gained significant attention in recent years due to its unique properties, including amphiphilicity, biocompatibility, and surfactant-like behavior.[15] TPGS can self-assemble into micelles in aqueous media, forming a hydrophobic core and a hydrophilic shell. This unique structure enables the encapsulation of poorly soluble drugs within the core, improving their solubility and stability.[16] Moreover, TPGS possesses inherent antitumor and chemo-sensitizing properties, making it an attractive carrier for anticancer drugs.[15] Pluronic copolymers, comprising poly(ethylene oxide)-poly(propylene oxide)-poly(ethylene oxide) (PEO-PPO-PEO) triblock structures, are another class of widely investigated micellar carriers.[17] These copolymers exhibit temperature-responsive sol–gel transition behavior, allowing them to undergo reversible micelle formation at body temperature. This property is advantageous for drug delivery applications, as it facilitates controlled drug release at the target site. Pluronic-based micelles have demonstrated promising results in enhancing drug solubility, improving cellular uptake, and prolonging drug circulation time.[18]

In this manuscript, we aimed to investigate the molecular mechanisms underlying ezetimibe's effects on cancer cells and explore the potential anticancer activity of ezetimibe loaded TPGS/Pluronic mixed micelles compared to single-component micelles against two human hormone-dependent breast cancer cell lines.

Materials and Methods

Materials

Ezetimibe was kindly gifted by the Saudi Arabian Japanese Pharmaceuticals Co. Ltd (SAJA) (Jeddah, KSA). Pluronic F127 was obtained from Xi'an Lyphar Biotech Co., Ltd (Xi'an, China). Ethanol and D-α- tocopherol polyethylene glycol 1000 succinate (TPGS) were purchased from Sigma-Aldrich (St. Louis, MI, USA). DMEM high glucose, fetal bovine serum (FBS), and cell culture antibiotics were obtained from Gibco, ThermoFisher Scientific (Waltham, MA, USA). Trypan blue, Thiazolyl Blue Tetrazolium, and Propidium Iodide were provided by Merck & Co., Inc. (West Point, PA, USA). The Annexin V-FITC Apoptosis Kit was given by Creative Biolabs (Shirley, NY, USA).

Preparation of Ezetimibe-Loaded Micelles/Mixed Micelles Formulations

The composition of the prepared polymeric micelles and mixed micelles formulation is illustrated in Table 1. Drug-to-polymer ratios of 1:10, 1:15, and 1:20 were used. TPGS and pluronic F127 1:1 molar ratio was utilized as previously described by Grimaudo et al[19]

To prepare pluronic F127 micelles formulation, the calculated amount of the polymer was dissolved in distilled water under continuous agitation using a magnetic stirrer to ensure uniform dispersion. Simultaneously, ezetimibe was solubilized in a minimal volume of ethanol, to prepare an ethanolic drug solution. The obtained ethanolic drug solution was added to the polymeric aqueous solution, and the mixture was left stirring overnight at room temperature until the complete evaporation of the organic solvent "ethanol". Finally, the obtained aqueous dispersion was subjected to filtration using a 0.22 µm pore size Millipore filter to remove un-entrapped drug and other impurities, resulting in a well-defined and stable pluronic F127 micelles formulation.

For TPGS micelles formulation, the drug and the polymer "TPGS" were dissolved in a minimal volume of ethanol. The obtained polymeric drug mixture was added to a specified volume of distilled water on a magnetic stirrer. Stirring continued overnight until complete evaporation of ethanol, and the mixture was filtered as described above.

For pluronic F127/TPGS mixed micelles formulation, a pluronic F127 aqueous solution and an ethanolic TPGS drug mixture were prepared as described above. The latter was added to the former, and the organic solvent "ethanol" was completely evaporated. Finally, the mixture was subjected to filtration.

Non-medicated nanocarrier formulations were also prepared for comparison purposes and to serve as a negative control in the cell line experiments. These formulations were assigned the same number followed by the letter "c" (F1c-F15c).

Characterization of the Prepared Formulation

Size, Polydispersity Index (PDI), and Zeta Potential

Malvern Zetasizer Nano ZSP of Malvern Panalytical Ltd. (Malvern, UK) was used to measure the size, PDI, and zeta potential of the prepared polymeric micelles and mixed micelles formulations. All measurements were conducted in triplicate without further dilution. Measurement of zeta potential was conducted at a scattering angle of 13° while maintaining a constant temperature of 25°C. To ensure accuracy, a 300-second equilibration period was allowed before the measurements. The entire process, including the number of runs, scan settings, voltage selection, and attenuation selection, was meticulously controlled and automated.

Table 1 Formulation Composition and Characterization of the Prepared Ezetimibe Nano-Micelles

	Composition				Characterization			
Run #	**Drug (mg)**	**TPGS (mg)**	**PF-127 (mg)**	**Polymer (%)**	**Size (nm)**	**PDI**	**ZP (mV)**	**EE (%)**
F1	50	500		1	92.34±6.56	0.42±0.11	−0.39±0.03	13.89 ± 0.29
F2	50	750		1.5	99±6.93	0.36±0.03	−0.09±0.14	25.32 ± 0.28
F3	50	1000		2	101.47±7.01	0.35±0.12	−7.23±1.13	27.86 ± 0.68
F4	50	2000		4	149.23±22.34	0.74±0.23	−2.16±0.04	90.87 ± 4.19
F5	50	3000		6	181.90±5.53	0.36±0.01	−1.49±0.31	94.03 ± 1.71
F6	50		500	1	34.01±2.00	0.37±0.26	−0.28±0.14	0.55 ± 0.14
F7	50		750	1.5	39.30±1.85	0.70±0.25	−2.60±0.83	1.14 ± 0.02
F8	50		1000	2	42.49±5.30	0.62±0.21	−0.35±0.17	1.25 ± 0.05
F9	50		2000	4	49.71±1.51	0.43±0.01	−2.24±0.55	2.23 ± 0.33
F10	50		3000	6	64.23±3.65	0.48±0.05	−1.49±0.31	6.47 ± 0.24
F11	50	53.6	446.4	1	153.73±7.23	0.40±0.08	−9.84±0.65	6.07 ± 0.08
F12	50	80.4	669.6	1.5	198.13±17.09	0.26±0.02	−5.93±0.76	10.73 ± 0.06
F13	50	107.2	892.8	2	224.22±10.07	0.17±0.06	−0.42±0.26	14.99 ± 0.07
F14	50	214.4	1785.6	4	241.05±8.98	0.31±0.03	−1.32±0.90	18.41 ± 1.15
F15	50	321.6	2678.4	6	278.34±9.11	0.46±0.07	−2.29±0.13	23.21 ± 3.44

Notes: Non-medicated formulations were also prepared and assigned the same number followed by the letter "c" (F1c-F15c). Polymer; TPGS and/or PF-127.

Entrapment Efficiency

To determine the percentage of entrapment efficiency (EE) for ezetimibe in the prepared formulations, the known volume of each formulation was taken and placed in a rounded bottom flask. The aqueous medium was completely evaporated under reduced pressure using Buchi Rotavapor R-200; BÜCHI Labortechnik AG (Flawil, Switzerland) at 50°C until formation of a dried film. Ten millilitres of ethanol were added to each sample that was thoroughly mixed and kept rotated in the Buchi Rotavapor for 10 minutes. Finally, each sample was measured spectrophotometrically at 235.4 nm against a blank of ethanol. The % EE was calculated using the following equation:

$$\%\ \mathrm{EE} = \frac{Amount\ of\ \ ezetimibe\ analyzed\ inthe\ sample}{Theoritical\ amount\ of ezetimibe\ in\ the\ same\ sample} \times 100$$

Morphological Studies Using Light and Transmission Electron Microscopies

Light microscopy and transmission electron microscopy (TEM) were used to study the morphological characteristics of the prepared nano-micelles formulations. Leica DM300 optical microscope (Wetzlar, Germany) equipped with HTC M8 digital camera was used. Photographs for the samples were taken at 40,000× magnification power. For TEM analysis, each studied formulation was mounted on a carbon coated grid and excess sample was removed using a filter paper. Each sample was left to dry and investigated using a high-resolution transmission electron microscopy of JEOL, JEM- 2100 (Tokyo, Japan).

Docking

Protein Preparation

The crystal structure of the human Interleukin-1 Beta Convertase with a peptide-based inhibitor, (3s)-N-Methanesulfonyl-3-({1-[N-(2-Naphtoyl)-L-Valyl]-L-Prolyl}Amino)-4-Oxobutanamide, was obtained from the Protein Data Bank (PDB ID: 1BMQ).[20] To prepare the protein for further analysis, we used the Protein Preparation Wizard in Maestro Schrödinger.[21] This involved adding missing hydrogen atoms to the residues, correcting metal ionization states, and removing water molecules beyond 5 Å. Additionally, appropriate charges were assigned to the protein, and restrained minimization was performed using the OPLS4 force field.

Ligand Preparation

For this study, we used Schrödinger's LigPrep tool[22] to dock the native reference, (3s)-N-Methanesulfonyl-3-({1-[N-(2-Naphthoyl)-L-Valyl]-L-Prolyl}Amino)-4-Oxobutanamide (PDB ID: MNO), and Ezetimibe. The OPSL3 force field was employed to energy-minimize the 3-dimensional structures of the compounds. Epik was used to generate all possible ionization states and tautomeric forms for each compound at a pH range of 7.0 ± 0.2, and hydrogen atoms were added accordingly. Furthermore, PROPKA was utilized to optimize hydrogen bonds, and water molecules located more than 3 Å away from the HET groups were excluded from consideration. These steps ensured the accuracy and reliability of our results while minimizing potential sources of error.

Covalent Docking

The Covalent Docking Tool in the Schrödinger suite[23] was employed to predict the reaction between 1BMQ and Ezetimibe. Cyc285 was selected as the reactive residue, allowing the ligand to react with it. The native ligand, MNO, was chosen to define the grid box. The type of reaction between Cyc285 and MNO was identified as a Michael reaction, which guided the selection of the reaction type when covalently docking Ezetimibe in 1BMQ.

Cell Viability Assay

MCF-7 and T47D cell lines were purchased from the American Type Culture Collection (Manassas, Virginia, USA) by King Fahd Medical Research Centre at KAU. Subsequently, these cells were generously donated to the Tissue Culture Unit within the Department of Biochemistry, Faculty of Science at KAU for conducting the cell line experiments in this study, following approval granted by the faculty's research ethics committee for their use. The selected human cell lines were cultured in DMEM media supplemented with 10% fetal bovine serum (FBS) and maintained in a CO_2 incubator at

37°C. When the cells reached 70–90% confluence, 5 mL of 0.25% trypsin was added to aid in cell detachment. The cells were then counted using Trypan blue staining, and the cell concentration was adjusted to 10^5 cells/mL. Subsequently, 100 µL of this cell suspension was added to each well of a 96-well plate, and the plate was incubated for 24 hours. The media in each well were then replaced with media containing different concentrations of ezetimibe, as well as formulations of nano-micelles labelled as F5, F10, and F15. The concentrations of ezetimibe ranged from 3.125 to 100 µg/mL, including both the free form and the form encapsulated within the nano-micelles. The corresponding amount of nano-micelle formulation without ezetimibe was used as a control and marked F5c, F10c, and F15c. In addition, various concentrations of cisplatin were used as positive controls. Each concentration was tested in triplicate. After 48 hours of further incubation at 37 °C, the media in each well was replaced with 100 µL of a 0.5 mg/mL MTT solution and incubated in the dark for 4 hours at 37°C. Following this, the MTT solution was replaced with 100 µL of dimethyl sulfoxide (DMSO), and the plate was allowed to sit for 15 minutes to dissolve the formazan crystals. The absorbance of each well was then measured at 595 nm using an ELISA reader (Japan- Bio-RAD microplate reader) to assess cell viability and determine the effects of the different treatments.[24,25]

The morphological alterations observed in the studied cell lines after treatment with the prepared formulations were studied using Nikon ECLIPSE Ti-S microscope, Nikon Instruments Inc. (Melville, NY, USA).

Evaluation of Apoptosis

Following the procedure outlined in the previous section, T47D cells were cultured for 24 hours and then detached using trypsin, which was subsequently neutralized with medium. The cells were counted, and each well of a 6-well plate was filled with 2 mL of medium containing 2×10^5 cells. The plate was allowed to incubate for 24 hours to enable the cells to proliferate and attach. The medium was then replaced with a new medium containing the IC_{50} concentration of ezetimibe, nano-micelles encapsulated with ezetimibe (F5), and nano-micelles loaded ezetimibe (F5c). After another 24-hour incubation time, 0.5 mL of 0.25% trypsin was added to each well of the plate. The plate was incubated for 5 minutes at 37°C, and the cells were collected and centrifuged. The pellets were washed twice with PBS. The pellet was suspended with 200 µL of binding buffer, and 25 µL Annexin V-FITC/propidium iodide (PI) of. The tubes were then allowed to incubate for 15 minutes. The cells were analyzed using a flow cytometer (Applied Biosystems, USA) with software that could detect apoptotic and necrotic cells.[26]

Evaluation of Cell Cycle

The T47D cells were treated in the same manner as stated in section 2.6, but with a higher number of cells (1×10^6 cells per well) added in a 6-well plate. The medium was replaced with a solution containing the IC_{50} level of ezetimibe, F5, and F5c. After 24 hours, the cells were taken from each well and washed with PBS twice. The cells were suspended in 300 µL of PBS and gradually treated with 0.7 mL of 100% ethanol before being placed at −20°C for at least an hour. Subsequently, the pelleted cells were treated with 25 µL of 50 µg/mL PI solution and 100 µL of PBS and left for one hour in the dark. PI attaches to DNA and forms cell aggregates at each stage of the cell cycle. The cells were then run through a flow cytometer (Applied Biosystems, USA) to determine the percentage of cells in each phase of the cell cycle.[27]

Statistical Analysis

The results are presented as an average with standard deviation in order to examine the formula properties and the viability of the treated cells. GraphPad Prism Software (version 9.0) was employed to determine the IC_{50} of the drug, and all data was subjected to statistical analysis. The flow cytometry software from Applied Biosystems was used to determine the percentage of cells in each phase, as well as the number of apoptotic and necrotic cells.

Results and Discussion

In this study, two different polymers were employed to develop the drug loaded formulations. Pluronic F12 which is a temperature-responsive polymer and TPGS which is a water-soluble form of vitamin E were used as they have been previously used to prepare nano-micelles formulations with different classes of hydrophobic drugs.[17,19,28–31] Selection of the minimum polymer concentration and the drug-to-polymer ratio were based on the critical micelle concentration

(CMC) for each polymer (pluronic F127 or TPGS) and that of the mixed micelles. Grimaudo et al mentioned a CMC for TPGS and pluronic F127 of 0.091 mM and 0.456 mM, respectively.[19] Also, they mentioned a CMC of mixed micelles for both polymers of 0.110 mM. Ahmed et al reported the same finding for TPGS micelles loaded with vinpocetine.[31]

Characterization of the Prepared Formulation

In the current study, the characterization of the prepared formulation was carried out meticulously using a range of essential parameters, namely size, polydispersity index (PDI), and zeta potential. These parameters are critical in evaluating the physical and chemical properties of the nano-formulation, and their assessment is pivotal in understanding the stability and performance. Size determination provides insights into the dimensions of the nanoparticles, helping us gauge their suitability for specific applications. The polydispersity index allows us to assess the uniformity or dispersity of particle sizes within the formulation, which is essential for ensuring consistent and reliable outcomes. Additionally, the zeta potential measurement offers valuable information on the surface charge of the nanoparticles, which plays a pivotal role in their stability and interactions with biological systems. Together, these characterizations provide a comprehensive understanding of the quality and potential of the prepared formulations for biomedical applications.

Results of the particle size revealed that all the prepared formulations were in the nano-size range (34.01 ± 2.00–278.34 ± 9.11) as illustrated in Table 1. Non-medicated formulations were slightly smaller in size than the corresponding medicated ones (data not shown). Pluronic-based formulations were smaller in size than TPGS-based formulations. Pluronic and TPGS have different HLB values, with Pluronic typically having a lower HLB than TPGS. Surfactants with lower HLB values tend to form smaller micelles due to their greater affinity for the hydrophobic core of the micelles. Moreover, Pluronic can form micelles more easily due to its block copolymer structure. The PEO blocks help solubilize hydrophilic compounds in the aqueous phase, while the PPO blocks form a hydrophobic core, resulting in smaller micelles. On the other hand, TPGS, although capable of micelle formation, may require a higher concentration or different conditions to achieve similar micelle sizes, as its structure combines a hydrophilic PEG chain with a lipophilic portion, which can impact self-assembly behavior. Alexandridis and Yang reported a similar explanation for micelle formation using pluronic block copolymer.[32]

The zeta potential of the prepared formulations was very close to zero, −0.09 ± 0.14 to −9.84 ± 0.65, which is attributed to the non-ionic nature of the polymers used to develop the formulation as previously mentioned.[19] It has been previously mentioned that a PDI value greater than 0.7 is an indication of a very broad particle size distribution.[33] The obtained PDI values were in the range 0.17 ± 0.06–0.74 ± 0.06 which indicate homogeneity of the particles and that the particle size distribution may vary. The lower end of the range (0.17) indicates a relatively narrow size distribution and a higher degree of homogeneity, while the higher end (0.74) suggests a wider distribution or less uniformity.

Entrapment efficiency was ranged from 0.55 ± 0.14–94.03 ± 1.71%. TPGS-based micelles formulations showed the highest ezetimibe EE%, while pluronic F127-based micelles formulations were the lowest. TPGS/pluronic F127 mixed micelles illustrated intermediate drug EE%. An explanation for this behaviour is the fact that while Pluronic F127 can form micelles, its structure and properties may not be as conducive to efficient encapsulation of ezetimibe when compared to TPGS. Moreover, the hydrophilic–lipophilic balance (HLB) of Pluronic F127 may not be as well suited to ezetimibe's hydrophobic nature, resulting in a lower drug EE%. Also, the bulky inner core of TPGS micelles formulation facilitates better retention of the drug inside the micelle core as previously mentioned.[34] Suksiriworapong et al reported a similar finding for diazepam-loaded polymeric micelles.[35] Combining TPGS and Pluronic F127 in a mixed micelle system can offer a balance between their individual properties. The mixture can potentially improve the solubilization and encapsulation of ezetimibe compared to using Pluronic F127 alone. This intermediate EE% indicates that the combination of TPGS and Pluronic F127 may optimize drug encapsulation to some extent, but it may not reach the high EE% achieved with TPGS alone. Islam et al reported an increase in the EE of ebastine from drug loaded poloxamer-188 and TPGS mixed micelles upon increasing the concentration of the micelles forming components. They also mentioned that the drug EE was in the range 26–82.1%.[36]

Morphological Studies

Figure 1 illustrates results for both transmission electron microscopy (TEM) and optical microscope images of micelles and mixed micelles formulations. Both techniques provide insights into the structural characteristics of these nanostructures. In TEM images, the micelles and mixed micelles formulation appear as well-defined, spherical nanoparticles with a uniform size distribution, indicative of their stable and homogeneous formation. On the other hand, optical microscope images provide valuable information regarding the overall appearance and spatial arrangement of these micelles, offering a complementary perspective to their structural analysis. These results collectively underscore the importance of precise characterization techniques in elucidating the properties and potential applications of this kind of formulation. It must be mentioned that since micelles are dynamic system and so accurate size determination is a complicated process as previously mentioned.[37]

Covalent Docking Studies

Following the preparation of Ezetimibe, we successfully performed covalent docking of its 3D structure into Interleukin-1 Beta Convertase (PDB ID: 1BMQ).

Notably, the native reference molecule (MNO) exhibited multiple hydrogen bonding interactions between the aldehyde and methyl sulfonyl amide groups with Cyc285 (2.02 Å), Gly238 (2.54 Å), and His237 (1.94 Å). Furthermore, a covalent bond formed between the thiol group of Cyc285 and the aldehyde group of the reference molecule (1.85 Å). Additionally, hydrophobic interactions were observed between MNO and the amino acids Ala284 and Cyc285 as illustrated in Figure 2.

Figure 3 displays the interaction of ezetimibe with the active protein. Ezetimibe displayed similar interactions as the native reference molecule with His237. However, Ezetimibe demonstrated additional interactions compared to MNO, including Pi–Pi stacking and Pi–cation interactions. Specifically, three hydrogen bonds were identified between the phenol, hydroxypropyl, and sulfanol groups of Ezetimibe with the amino acids Pro177 (1.68 Å), Gln283 (1.93 Å), and Arg179 (2.8 Å), respectively. Moreover, the imidazole group of His237 exhibited Pi–Pi stacking with the hydroxyphenyl group of Ezetimibe (4.15 Å), while the guanidino group of Arg179 interacted with the fluorophenyl part of Ezetimibe through a Pi–cation interaction. Cyc285 successfully formed a covalent bond with the azetidinol group of Ezetimibe (1.82 Å), mirroring its interaction with the native reference molecule.

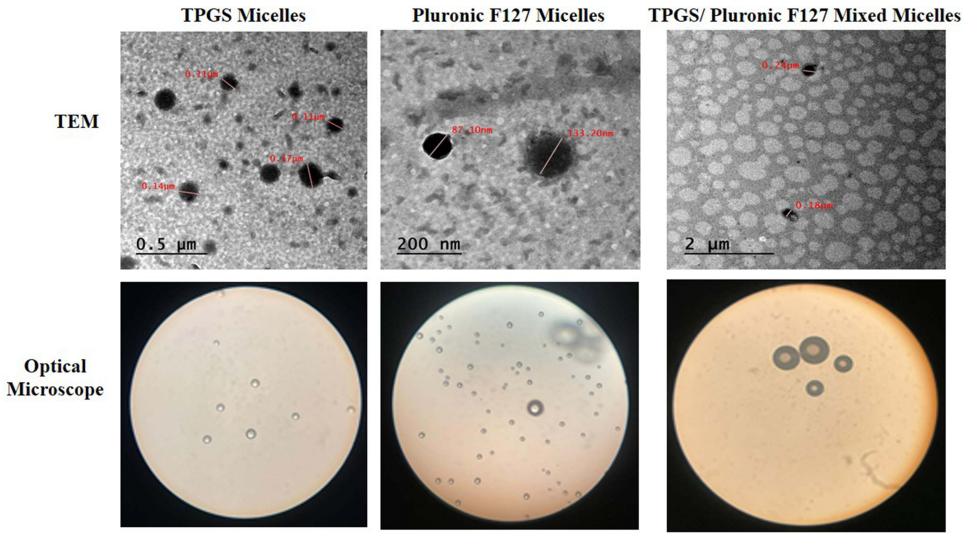

Figure 1 Transmission electron microscope and optical microscopic images for the prepared micelles and mixed micelles formulations.

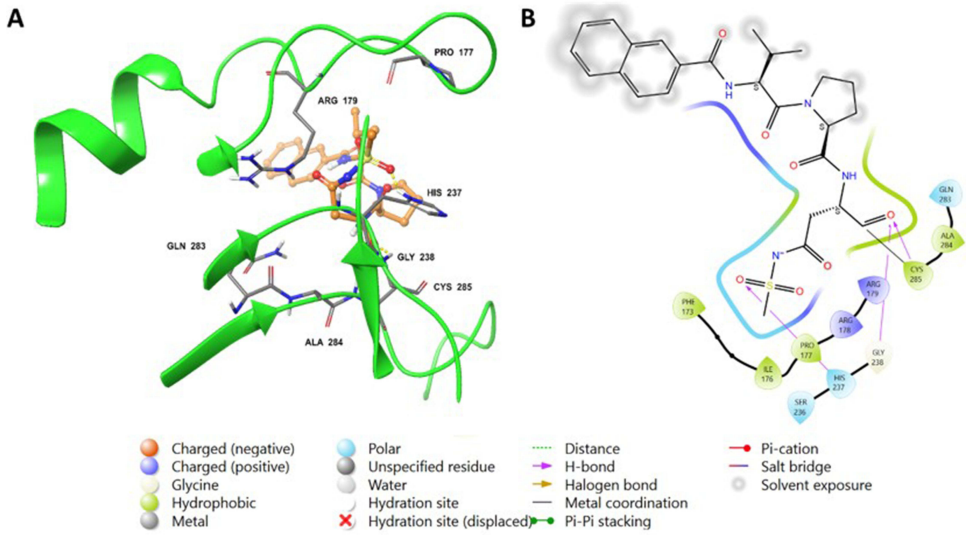

Figure 2 The binding mode of the native agonist, (3s)-N-Methanesulfonyl-3-({1-[N-(2-Naphthoyl)-L-Valyl]-L-Prolyl}Amino)-4-Oxobutanamide (PDB-ID: MNO), in the active site of Interleukin-1 Beta Convertase (PDB-ID: 1BMQ) is depicted. Panel (**A**) shows the 3D representation of the complex between 1BMQ and MNO, with MNO displayed as Orange sticks. The figure also highlights hydrogen bonds (yellow dotted lines) and ionic bonds (blue dotted lines). Panel (**B**) presents a 2D depiction of the same complex.

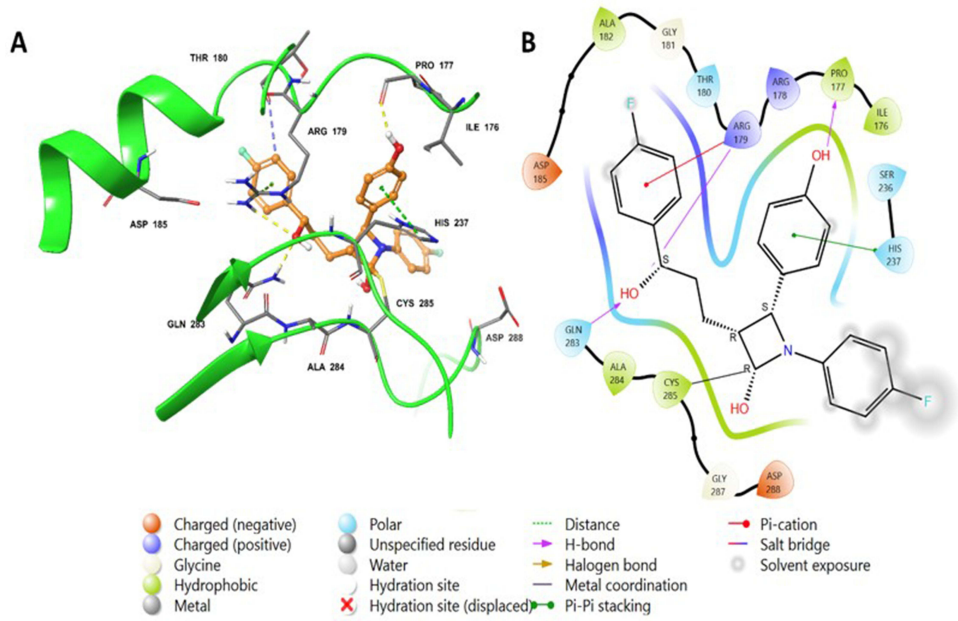

Figure 3 The proposed binding mode of Ezetimibe in the active site of Interleukin-1 Beta Convertase (PDB-ID: 1BMQ) is depicted. Panel (**A**) showcases the 3D representation of the complex between 1BMQ and Ezetimibe, with Ezetimibe represented as Orange sticks. The figure also illustrates hydrogen bonds (depicted as yellow dotted lines) and ionic bonds (represented by blue dotted lines). Panel (**B**) presents a 2D depiction of the same complex.

Anti-Tumour Activity

The IC_{50} of free ezetimibe and ezetimibe encapsulated in nano-micelles against MCF-7 and T47D cell lines was determined. The percentage of cell viability was evaluated after treating the studied cells with different concentrations of both free and loaded ezetimibe for 48 hours. The viability of the cells treated with ezetimibe and the prepared formulations were compared with those treated with cisplatin as a positive control. IC_{50} values of ezetimibe for MCF-7 and T47D were found to be 17.6 and 19.5 μg/mL, respectively. When compared to cisplatin, the IC_{50} values of ezetimibe

were 2.7 and 3.3 times higher in MCF-7 and T47D, respectively. Different preparations of nano-micelles (F5, F10, and F15) encapsulating ezetimibe showed IC_{50} values of 4.5, 6.16, and 12.96 µg/mL in MCF-7, and 8.2, 16.7, and 34.9 µg/mL in T47D, respectively. In MCF-7, the IC_{50} values of F5, F10, and F15 were reduced by 2.9, 4.2, and 2.1 folds in comparison to the formulations without ezetimibe (F5c, F10c, and F15c, respectively). In T47D, the IC50 values of F5, F10, and F15 were also decreased by 4.2, 1.6, and 1.2 folds, respectively, in comparison to their corresponding formulations without ezetimibe. Furthermore, the IC_{50} value of F5 in MCF-7 was 1.44 times less than the IC_{50} of cisplatin, while in T47D, it was 1.4 times higher (Figures 4 and 5, Table 2).

Ezetimibe is mostly known as an oral medicine used to treat high blood cholesterol levels. Ezetimibe suppresses cancer cell growth and proliferation via affecting the cholesterol metabolism. The blockage of the mevalonate pathway, which is necessary for cell growth and survival, is how ezetimibe exerts its anticancer impact.[4] Ezetimibe has the potential to limit cancer formation and progression by anti-angiogenesis, anti-inflammation, and immunological boosting.[3] Niemann-Pick C1-Like 1 (NPC1L1) is a transmembrane protein that is required for cholesterol absorption in the intestine. Ezetimibe inhibits the expression of this protein (NPC1L1). Increased NPC1L1 expression has been linked to colorectal cancer (CRC) formation and serves as a biomarker for CRC, and ezetimibe may lessen the risk of CRC.[38] Several laboratory and human clinical trials carried out in the last ten years have offered additional evidence supporting the idea that ezetimibe could be a viable alternative for cancer therapy and prevention. However, there is currently a lack of data demonstrating ezetimibe-specific effects on cancer human cell lines, including its efficacy in causing programmed cell death and phases of the cell cycle.

The IC_{50} of MCF-7 and T47D breast cancer cells treated with ezetimibe formulated in TPGS nano-micelles was shown to be the lowest when compared to treatment with ezetimibe alone, drug-loaded PF127 micelles, or drug-loaded TPGS and PF127 mixed micelles. This formulation "drug loaded TPGS micelle" was shown to be the most successful in eliciting anticancer activity in MCF-7 (ER+) and T47D (ER+ and PR+) cells, therefore it was chosen for further investigation of the percentage of apoptotic cells and cell cycle phases in T47D treated with ezetimibe alone or ezetimibe encapsulated in TPGS. Accordingly, successful ezetimibe release from the prepared drug-loaded nanocarrier formulation

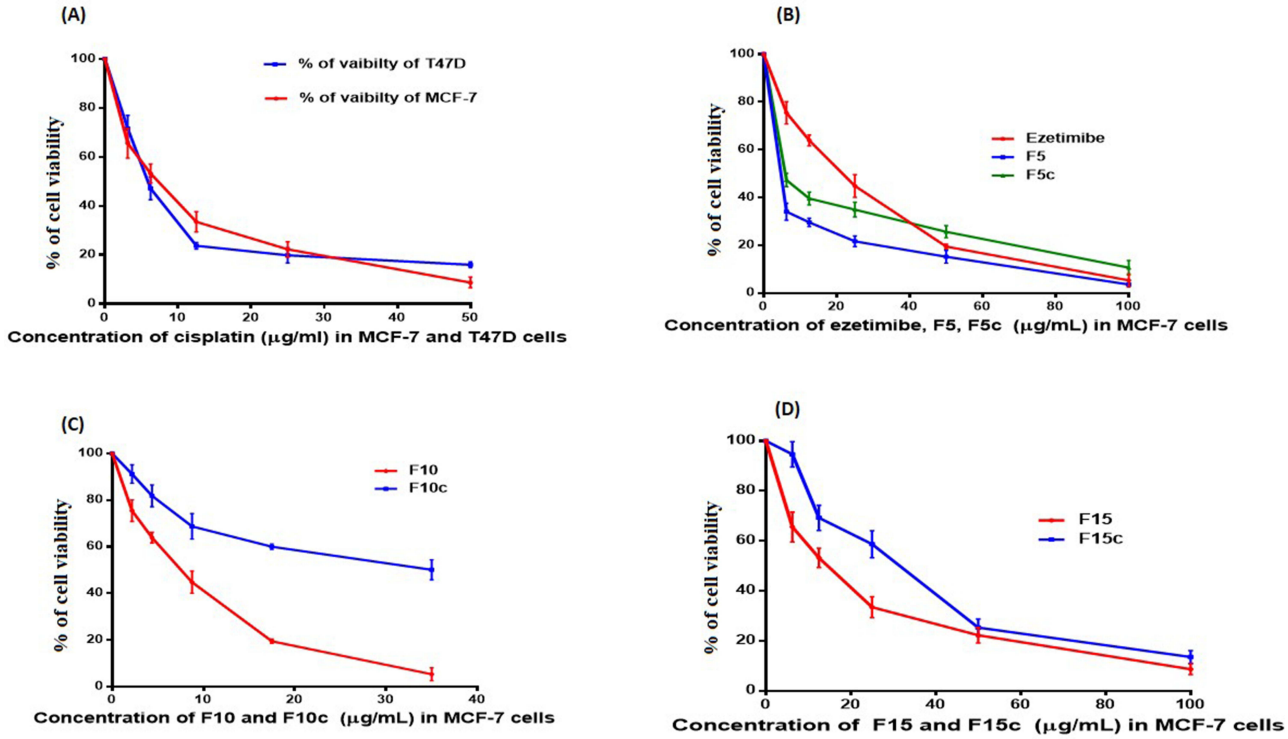

Figure 4 Cell viability of MCF-7 and T47D after treatment with varying concentrations of cisplatin (**A**) and viability of MCF-7 treated with ezetimibe and nano-micelles formulations F5 and F5c (**B**), F10 and F10c (**C**), and F15 and F15c (**D**).

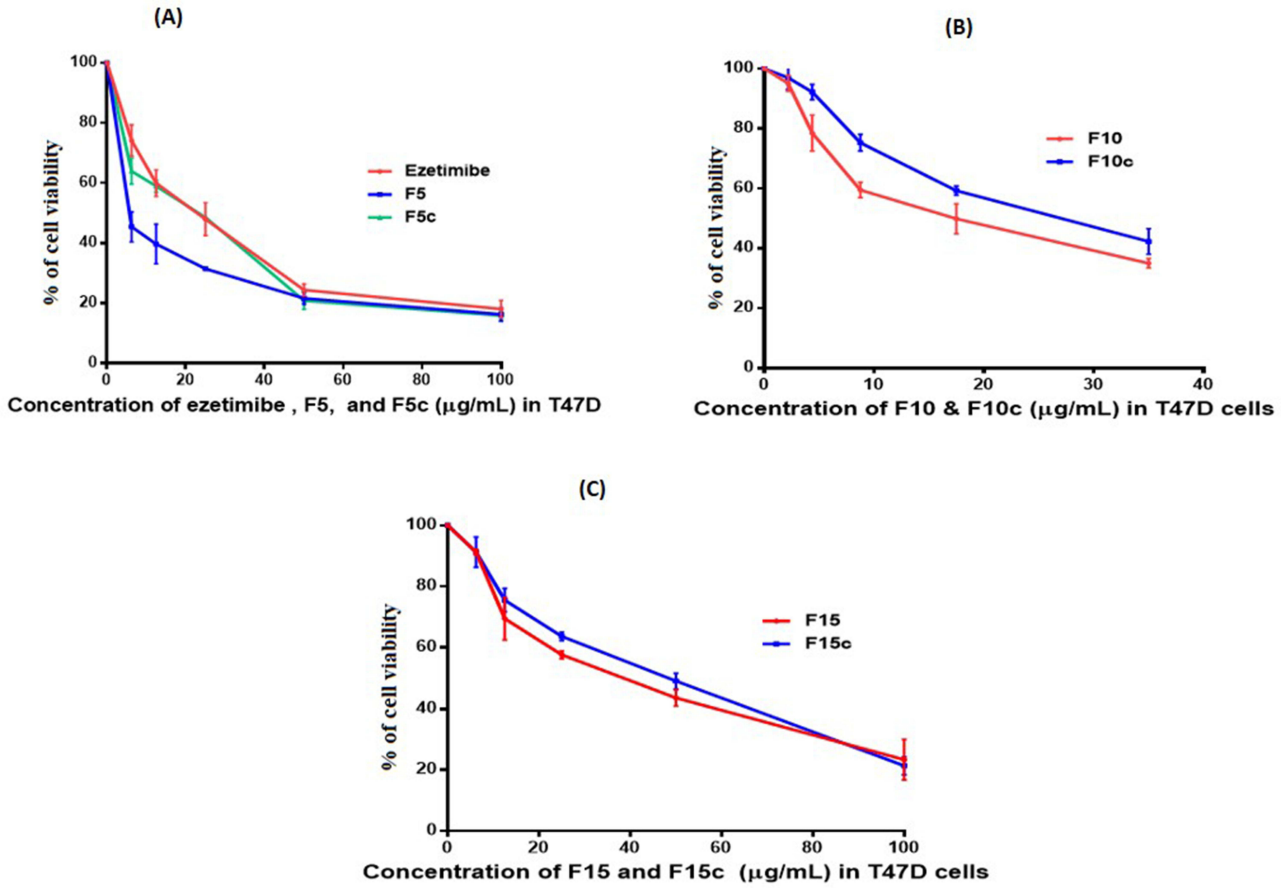

Figure 5 Cell viability of T47D after treatment with various doses of with ezetimibe-loaded nano-micelles formulations F5 and F5c (**A**), F10 and F10c (**B**), and F15 and F15c (**C**).

was indicated from the marked reduction in the percentage of cell viability obtained from this formulation when compared to the pure drug and non-medicated nanocarrier formulation as shown in Figure 4. Targeting the tumour cells and avoiding direct effect on normal tissues will be the focus of our upcoming study by investigating various

Table 2 IC_{50} of Ezetimibe and the Prepared Nano-Micelle Formulations on Human Breast Cell Lines (MCF-7 and T47D) After 48 Hours

Cells / Treatment	MCF-7 cell line		T47D cell line	
	Range (µg/mL)	Value (µg/mL)	Range (µg/mL)	Value (µg/mL)
Cisplatin	5.797–7.245	6.48	4.909–6.984	5.855
Ezetimibe	14.61–21.20	17.6	17.26–22.04	19.51
F5	3.621–5.617	4.51	6.325–10.68	8.218
F10	5.113–7.421	6.16	14.34 −19.48	16.71
F15	11.59–14.49	12.96	30.09–40.44	34.89
F5c	6.866–11.47	8.873	14.11–20.08	16.83
F10c	22.07–31.50	26.37	24.04–31.51	27.52
F15c	21.11–35.73	27.46	35.51–47.78	41.19

strategies that enhance the specificity of drug release to tumor cells, such as incorporating targeting ligands or utilizing the unique microenvironment of tumors (eg, acidic pH or overexpressed receptors).

Apoptosis and Necrosis of T47D Treated Cells

In this experiment, we selected IC_{50} values for ezetimibe, F5, and F5c, with doses of 20 µg/mL, 10 µg/mL, and a volume equivalent to 35 µg/mL, respectively. The percentage of T47D cells in late apoptosis after treatment with ezetimibe, F5, and F5c was found to be 40%, 43.9%, and 34.9%, respectively. No early apoptosis was observed in T47D cells treated with ezetimibe, F5, or F5c. The percentage of necrosis in T47D cells treated with ezetimibe, F5, and F5c was ranged from 7.9% to 11% (Figure 6).

Cell Cycle Analysis of T47D-Treated Cells

Unlike the untreated T47D cells that were arrested in sub G1 (8.5%), G0/G1 phase (48.5%), S phase (20.3%), and G2/M (22.7%), respectively, T47D cells treated with ezetimibe at a dose of 20 µg/mL showed an increase in sub G1 (27.9%), a decrease in G0/G1 phase (33.4%), and nearly the same in S phase (22.1%) and a decrease in G2/M (16.1%) as illustrated in Figure 7A and B, Figure 8.

T47D cells treated with 10 µg/mL of ezetimibe loaded nano-micelle (F5) and a volume equivalent to 35 µg/mL of the non-medicated nano-micelle showed a significant increase in sub G1 (14.8%, 14.8%), a slight decrease in G1/G0 (46.8, 46.3%), nearly the same in S phase (22.1, 20.1%), and also nearly the same in G2/M phases (18.0 and 20.8%) when compared to untreated T47D cells (Figure 7C and D, Figure 8).

It has been previously reported that ezetimibe arrests cells in the G0/G1 phase by inhibiting the production of cyclin D1, a protein linked to cancer growth. This is accomplished by inhibiting the MAPK signalling system, which controls gene expression, cell proliferation, and survival. If MAPK signalling is uncontrolled, it can lead to uncontrolled cell

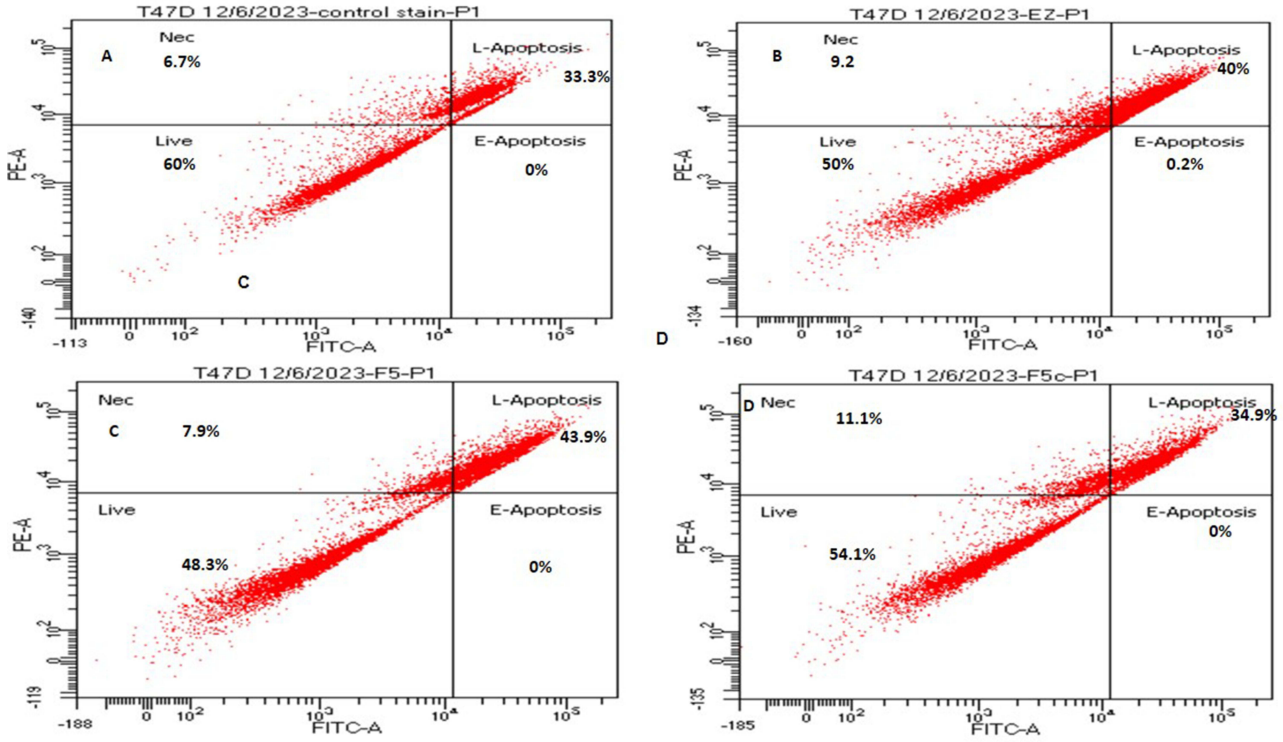

Figure 6 T47D staining with Annexin V/7-PI; control (**A**); cells treated with 20 µg/mL ezetimibe (**B**); cells treated with 5 µg/mL ezetimibe formulated in nano-micelles [F5] (**C**); and cells treated with an equivalent IC_{50} volume of non-medicated formulation [F5c] (**D**).

Notes: % of viable cells in the first quarter (lower left); the second quarter (upper left) represents the percentage of necrosis; the third quarter (lower right) represents the percentage of early apoptosis; and the fourth quarter (upper right) represents the percentage of late apoptosis.

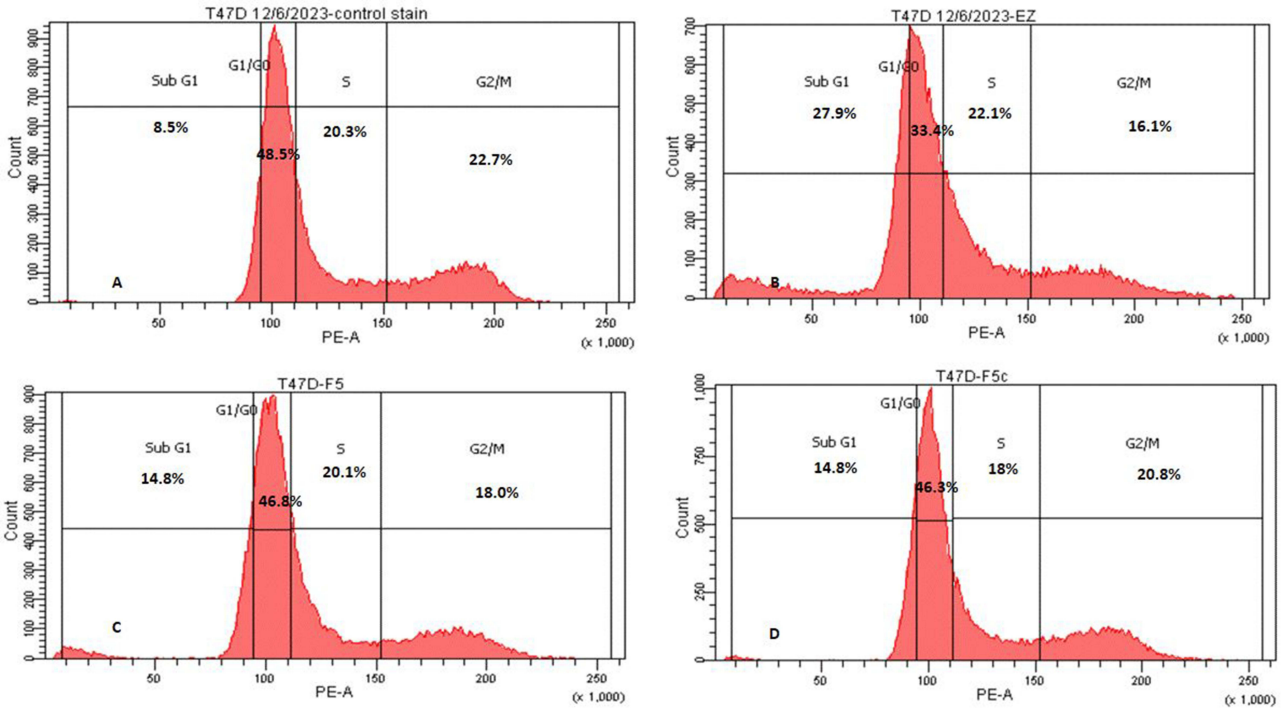

Figure 7 Cycle arrest of untreated T47D (**A**) and cells treated with 20 µg/mL ezetimibe (**B**); cells treated with 5 µg/mL ezetimibe formulated in nano-micelles [F5] (**C**); and cells treated with an equivalent IC_{50} volume of non-medicated formulation [F5c] (**D**).

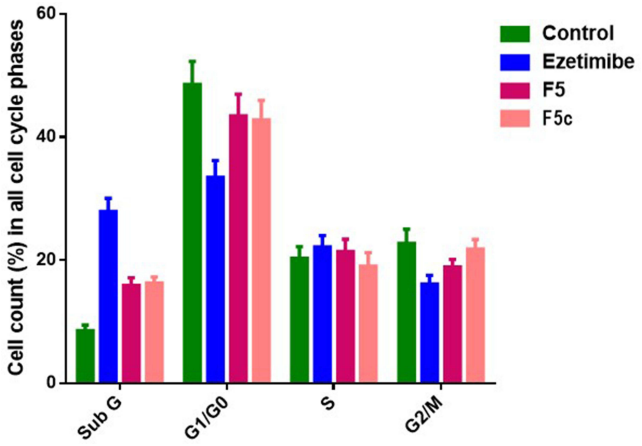

Figure 8 Percentage of cells across different phases of the cell cycle in T47D cells treated with EZ, F5, and F5c.

growth and apoptosis resistance.[39] Ezetimibe, F5, and F5c cause an increase in the proportion of cells undergoing apoptosis, leading to the accumulation of cells in the subG0 phase of the cell cycle.

Cell Morphology of T47D-Treated Cells

Figure 9 illustrates the morphological changes in T47D cells. Treatment of the cells with ezetimibe resulted in a change in shape and a reduction in the number of the studied cells when compared to untreated cells. Marked changes in the cell morphology and in the number of surviving cells were noticed following treatment with F5 despite using the lowest concentration of this formulation. These microscopic observations deepen our understanding of the cellular responses to the treatments (Figure 9). Similar finding was reported for the change in the morphology of HepG2 cells following

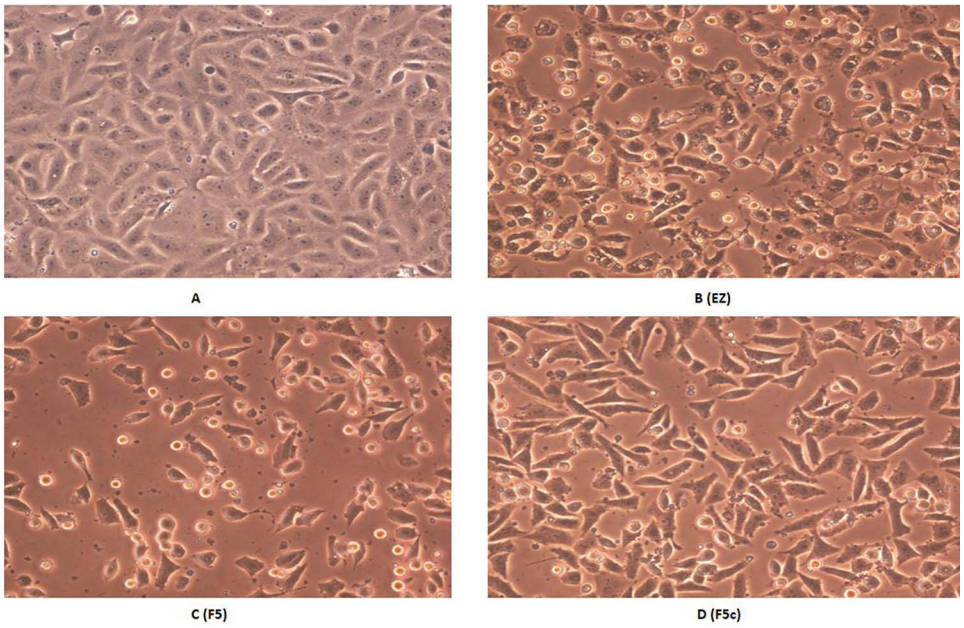

Figure 9 Morphology of the untreated T47D cells (**A**) and cells treated with 20 µg/mL ezetimibe (**B**), cells treated with 5 µg/mL ezetimibe formulated in nano-micelles [F5] (**C**), and cells treated with an equivalent IC_{50} volume of non-medicated formulation [F5c] (**D**). The cells were observed at 20× magnification power.

treatment with pure 6-mercaptopurine, drug loaded self-nanoemulsifying drug delivery system formulation, and non-medicated formulation.[40]

Conclusion

The potential of ezetimibe, a well-established cholesterol-lowering drug, as an emerging candidate for enhancing anticancer activity through the development of drug TPGS/Pluronic F12 nano-micelle formulations has been explored. Molecular docking study illustrated proposed binding mode of ezetimibe in the active site of Interleukin-1 Beta Convertase. Ezetimibe encapsulated in the TPGS micelles formulation demonstrated promising anticancer activities due to its capacity to arrest cell cycle at subG1 due to DNA damage causing apoptosis in the lowest of IC_{50} of both human breast cell carcinoma (MCF-7 and T47D). A comprehensive formulation and characterization study including stability testing aimed at developing an optimized ezetimibe dosage form, such as injectable, transdermal, and oral dosage forms, integrated with the promising TPGS nano-micelles formulation is crucial. Furthermore, investigating the pharmacokinetics of this newly formulated dosage form is imperative. This systematic approach will be pivotal in comprehensively understanding and optimizing the potential of the TPGS nano-micelles as a delivery system for ezetimibe, ultimately contributing to the development of an advanced and effective pharmaceutical formulation. Finally, more research is required to determine the signaling pathways that reduce the inhibitory effects of ezetimibe encapsulated TPGS on human cancer cell lines and models in rats.

Acknowledgments

This research work was funded by Institutional Fund Projects under grant no. (IFPIP: 218-166-1443). The authors gratefully acknowledge technical and financial support provided by the Ministry of Education and King Abdulaziz University, DSR, Jeddah, Saudi Arabia.

Disclosure

The authors report no conflicts of interest in this work.

References

1. Nutescu EA, Shapiro NL. Ezetimibe: a selective cholesterol absorption inhibitor. *Pharmacotherapy*. 2003;23:1463–1474. doi:10.1592/phco.23.14.1463.31942
2. Garcia-Calvo M, Lisnock J, Bull HG, et al. The target of ezetimibe is Niemann-Pick C1-Like 1 (NPC1L1). *Proc Natl Acad Sci USA*. 2005;102:8132–8137. doi:10.1073/pnas.0500269102
3. Gu J, Zhu N, Li H-F, et al. Ezetimibe and Cancer: is There a Connection? *Front Pharmacol*. 2022;13. doi:10.3389/fphar.2022.831657
4. Solomon KR, Pelton K, Boucher K, et al. Ezetimibe Is an Inhibitor of Tumor Angiogenesis. *Am J Pathol*. 2009;174:1017. doi:10.2353/ajpath.2009.080551
5. Soulele K, Karalis V. Development of a joint population pharmacokinetic model of ezetimibe and its conjugated metabolite. *Eur J Pharm Sci*. 2019;128:18–26. doi:10.1016/j.ejps.2018.11.018
6. Aukunuru J, Nanam P, Rambabu B, Sailu C, Thadkala K. Preparation and characterization of amorphous ezetimibe nanosuspensions intended for enhancement of oral bioavailability. *Int J Pharm Investig*. 2014;4:131. doi:10.4103/2230-973X.138344
7. Bali V, Ali M, Ali J. Novel nanoemulsion for minimizing variations in bioavailability of ezetimibe. *J Drug Target*. 2010;18:506–519. doi:10.3109/10611860903548362
8. Agrawal YO, Mahajan UB, Agnihotri VV, et al. Ezetimibe-loaded nanostructured lipid carrier based formulation ameliorates hyperlipidaemia in an experimental model of high fat diet. *Mol*. 2021;26:1485. doi:10.3390/molecules26051485
9. Shukr MH, Ismail S, Ahmed SM. Development and optimization of ezetimibe nanoparticles with improved antihyperlipidemic activity. *J Drug Deliv Sci Technol*. 2019;49:383–395. doi:10.1016/j.jddst.2018.12.001
10. Shaw SM, Najam O, Khan U, et al. Ezetimibe and atorvastatin both immunoregulate CD4+ T cells from cardiac transplant recipients in vitro. *Transpl Immunol*. 2009;21:179–182. doi:10.1016/j.trim.2009.03.001
11. Pelton K, Coticchia CM, Curatolo AS, et al. Hypercholesterolemia induces angiogenesis and accelerates growth of breast tumors in vivo. *Am J Pathol*. 2014;184:2099–2110. doi:10.1016/j.ajpath.2014.03.006
12. Nicolle R, Blum Y, Marisa L, et al. Pancreatic adenocarcinoma therapeutic targets revealed by tumor-stroma cross-talk analyses in patient-derived xenografts. *Cell Rep*. 2017;21:2458–2470. doi:10.1016/j.celrep.2017.11.003
13. Yang L, Sun J, Li M, et al. Oxidized low-density lipoprotein links hypercholesterolemia and bladder cancer aggressiveness by promoting cancer stemness. *Cancer Res*. 2021;81:5720–5732. doi:10.1158/0008-5472.CAN-21-0646
14. Wang Y, You S, Su S, et al. Cholesterol-lowering intervention decreases mTOR Complex 2 signaling and enhances antitumor immunity. *Clin Cancer Res*. 2022;28:414–424. doi:10.1158/1078-0432.CCR-21-1535
15. Yang C, Wu T, Qi Y, Zhang Z. Recent advances in the application of vitamin E TPGS for drug delivery. *Theranostics*. 2018;8:464–485. doi:10.7150/thno.22711
16. Guo Y, Luo J, Tan S, Otieno BO, Zhang Z. The applications of Vitamin e TPGS in drug delivery. *Eur J Pharm Sci*. 2013;49:175–186. doi:10.1016/j.ejps.2013.02.006
17. Zhao L, Du J, Duan Y, et al. Curcumin loaded mixed micelles composed of Pluronic P123 and F68: preparation, optimization and in vitro characterization. *Colloids Surfaces B Biointerfaces*. 2012;97:101–108. doi:10.1016/j.colsurfb.2012.04.017
18. Naharros-Molinero A, Caballo-González MÁ, de la Mata FJ, García-Gallego S. Direct and reverse pluronic micelles: design and characterization of promising drug delivery nanosystems. *Pharmaceutics*. 2022;14:2628. doi:10.3390/pharmaceutics14122628
19. Grimaudo MA, Pescina S, Padula C, et al. Poloxamer 407/TPGS mixed micelles as promising carriers for cyclosporine ocular delivery. *Mol Pharm*. 2018;15:571–584. doi:10.1021/acs.molpharmaceut.7b00939
20. Okamoto Y, Anan H, Nakai E, et al. Peptide based interleukin-1 beta converting enzyme (ICE) inhibitors: synthesis, structure activity relationships and crystallographic study of the ICE-inhibitor complex. *Chem Pharm Bull*. 1999;47:11–21. doi:10.1248/cpb.47.11
21. Tavella D, Ouellette DR, Garofalo R, et al. A novel method for in silico assessment of Methionine oxidation risk in monoclonal antibodies: improvement over the 2-shell model. *PLoS One*. 2022;17:e0279689. doi:10.1371/journal.pone.0279689
22. LigPrep. Schrödinger. New York, NY, USA: LLC; 2021. Available from: https://www.schrodinger.com/products/ligprep. Accessed November 11, 2023.
23. Glide. Schrödinger. New York, NY, USA: LLC; 2021. Available from: https://www.schrodinger.com/products/glide. Accessed November 11, 2023.
24. van Meerloo J, Kaspers GJL, Cloos J. Cell sensitivity assays: the MTT assay. *Methods Mol Biol*. 2011;731:237–245.
25. Ali EMM, Elashkar AA, El-Kassas HY, Salim EI. Methotrexate loaded on magnetite iron nanoparticles coated with chitosan: biosynthesis, characterization, and impact on human breast cancer MCF-7 cell line. *Int J Biol Macromol*. 2018;120:1170–1180. doi:10.1016/j.ijbiomac.2018.08.118
26. Kumar R, Saneja A, Panda AK. An annexin V-FITC-propidium iodide-based method for detecting apoptosis in a non-small cell lung cancer cell line. *Methods Mol Biol*. 2021;2279:213–223.
27. Fried J, Perez AG, Clarkson BD. Flow cytofluorometric analysis of cell cycle distributions using propidium iodide. Properties of the method and mathematical analysis of the data. *J Cell Biol*. 1976;71:172–181. doi:10.1083/jcb.71.1.172
28. Basak R, Bandyopadhyay R. Encapsulation of hydrophobic drugs in pluronic F127 micelles: effects of drug hydrophobicity, solution temperature, and pH. *Langmuir*. 2013;29:4350–4356. doi:10.1021/la304836e
29. Meng X, Liu J, Yu X, et al. Pluronic F127 and D-α-tocopheryl polyethylene glycol succinate (TPGS) mixed micelles for targeting drug delivery across the blood brain barrier. *Sci Rep*. 2017;7:2964. doi:10.1038/s41598-017-03123-y
30. Ahmed OAA, El-Say KM, Aljaeid BM, Badr-Eldin SM, Ahmed TA. Optimized vinpocetine-loaded vitamin E D- α - tocopherol polyethylene glycol 1000 succinate- alpha lipoic acid micelles as a potential transdermal drug delivery system: in vitro and ex vivo studies. *Int J Nanomedicine*. 2019;14:33–43. doi:10.2147/IJN.S187470
31. Ahmed TA, El-Say KM, Ahmed OA, Aljaeid BM. Superiority of TPGS-loaded micelles in the brain delivery of vinpocetine via administration of thermosensitive intranasal gel. *Int J Nanomedicine*. 2019;14:5555–5567. doi:10.2147/IJN.S213086
32. Alexandridis P, Lin Y. SANS investigation of polyether block copolymer micelle structure in mixed solvents of water and formamide, ethanol, or glycerol. *Macromolecules*. 2000;33:5574–5587. doi:10.1021/ma000332o
33. Ahmed TA, Alay AMS, Okbazghi SZ, Alhakamy NA. Two-step optimization to develop a transdermal film loaded with dapoxetine nanoparticles: a promising technique to improve drug skin permeation. *Dose-Response*. 2020;18:1559325820923859. doi:10.1177/1559325820923859

34. Mu L, Elbayoumi TA, Torchilin VP. Mixed micelles made of poly(ethylene glycol)-phosphatidylethanolamine conjugate and d-alpha-tocopheryl polyethylene glycol 1000 succinate as pharmaceutical nanocarriers for camptothecin. *Int J Pharm*. 2005;306:142–149. doi:10.1016/j.ijpharm.2005.08.026
35. Suksiriworapong J, Rungvimolsin T, A-Gomol A, Junyaprasert VB, Chantasart D. Development and characterization of lyophilized diazepam-loaded polymeric micelles. *AAPS Pharm Sci Tech*. 2014;15:52–64. doi:10.1208/s12249-013-0032-4
36. Islam N, Irfan M, Khan S-U-D, et al. Poloxamer-188 and d-α-tocopheryl polyethylene glycol succinate (TPGS-1000) mixed micelles integrated orodispersible sublingual films to improve oral bioavailability of ebastine; in vitro and in vivo characterization. *Pharmaceutics*. 2021;13:1–21. doi:10.3390/pharmaceutics13010054
37. Franken LE, Boekema EJ, Stuart MCA. Transmission electron microscopy as a tool for the characterization of soft materials: application and interpretation. *Adv Sci*. 2017;4. doi:10.1002/advs.201600476
38. Kwon RJ, Park E-J, Lee SY, et al. Expression and prognostic significance of Niemann-Pick C1-Like 1 in colorectal cancer: a retrospective cohort study. *Lipids Health Dis*. 2021;20. doi:10.1186/s12944-021-01539-0
39. Li Q, Yang Y-B, Yang Y-X, et al. Inhibition of smooth muscle cell proliferation by ezetimibe via the cyclin D1-MAPK pathway. *J Pharmacol Sci*. 2014;125:283–291. doi:10.1254/jphs.13239FP
40. Ahmed TA, Ali EMM, Kalantan AA, Almehmady AM, El-Say KM. Exploring the enhanced antiproliferative activity of turmeric oil and 6-mercaptopurine in a combined nano-particulate system formulation. *Pharmaceutics*. 2023;15:1901. doi:10.3390/pharmaceutics15071901